

Multi-wavelet Feature Extraction Method for Variable Illumination Face Recognition

Fei Guo

Modern Education Technology Center
Qingdao Technological University
Qingdao, 266520, P. R. China
guofei_qd@163.com

Hui Wang

College of Communication and Electronic Engineering
Qingdao Technological University
Qingdao, 266033, P. R. China
972482380@qq.com

Received February, 2015; revised July, 2015

ABSTRACT. *A face recognition method based on the logarithm restoration algorithm and the multi-wavelet LH features is proposed in this paper to solve the variable illumination problem. By analyzing the model of variable illumination face images, all multi-wavelet frequency band features and their frequency amplitudes of the preprocessed image by the logarithm and normalization computation, it can be seen that the multi-wavelet LH features can present the detail features of the face image better. Thus, the face image is calculated by the logarithm and normalization operations firstly, which change the multiplicative noise to the additive noise and can reduce the illumination effects effectively. And then the multi-wavelet LH features are obtained by filtering every row and every column of the preprocessed image using the multi-wavelet low pass filter and the multi-wavelet high pass filter sequentially. At last, the test face image is identified using the nearest neighborhood method. The experimental results based on the extended Yale B and CMU PIE Pose C09 databases show that the proposed method can obviously improve the face recognition effectiveness with a good robustness.*

Keywords: Face recognition, Feature extraction, Multi-wavelet, Multi-wavelet LH features.

1. Introduction. Illumination change is one of the most important factors that affect the face recognition performance. On one hand, the illumination change may enhance some parts of the face image; On the other hand, the face image may be blurred or even invisible because the variable illumination may shield some parts of the face, which may reduce the face recognition rate. Shan et al. [1] proposed an illumination normalization algorithm based on wavelets, which processes the original face image's wavelet decomposition coefficients by using different methods for different bands. The image after illumination reduction is obtained by reconstructing the processed wavelet coefficients, which are multiplied by a factor larger than 1 in the high frequency band and processed using the histogram method in the low frequency band. Goh et al. [2] gave an illumination invariable preprocessing method based on wavelets, in which the low frequency band wavelet coefficients of the image's logarithm values are set to 0, and the reduced illumination image is reconstructed with the modified low frequency coefficients and the

unchanged high frequency coefficients. Both above methods thought that the illumination change mainly affects the low frequency band. In fact, the edge of shadows caused by the illumination will introduce the high frequency information. Cao et al. [3,4] improved the recognition effectiveness by an illumination invariable face recognition method using the wavelet transform with a denoising model, in which the illumination invariable features are extracted and the edge features are enhanced by processing the high frequency coefficients. Nie et al. [5] proposed a logarithm domain illumination compensated face recognition method based on the wavelet packet transform. Both Cao et al. and Nie et al. viewed the horizontal, vertical and diagonal detail frequency band components as the equal position without considering their differences and roles in the face recognition process.

According to the illumination model[6], the illumination effects can be thought as a multiplicative noise for the original image. One of the best methods to processing the multiplicative noise is changing the multiplicative noise into an additive noise by logarithm computation, which can weaken the effect of the noise and make the following processes easy. Therefore, we first calculate the logarithm value of the original image corrupted by illumination, and then intently choose the appropriate filter to filter the illumination effects by considering the spectrum distribution of the noise image. The wavelet transform has good multi-resolution property, which can present the image feature in one hand, and easily filter the noise using different processing methods in different frequency band. Compared with the scalar wavelet, the multi-wavelet analysis has the symmetry, orthogonality, compact support and high vanishing moments at the same time and has more excellent performance in presenting the object. Zhou et al [8] proposed a face recognition method based on multi-wavelet and sparse representation and illustrated the priority of the multi-wavelet. So we choose the multi-wavelet analysis to process the image after logarithm computation. We can get four frequency band components by decomposing the preprocessed image once. Since we use the low or high multi-wavelet filter to the image's row and column sequentially, we call them LL, LH, HL, HH components. By analyzing the four components' features, their reconstructed images obtained only using every component respectively and their corresponding spectrum, we found that the multi-wavelet LH component of the face can present the detail information of the face and reduce the illumination effects better. Thus, this paper presents a face recognition approach based on the logarithm computation and the multi-wavelet LH component feature. The experiments are performed on the extended Yale B and CMU PIE Pose C09 face databases with various illumination changes. The results show that the proposed approach can improve the recognition rate apparently compared with the methods using the original data, the logarithm method, the LL and HL component features, the LL+sparse method [8] and the logarithm computation+wavelet method [4] respectively. And it also has better robustness.

The rest of this paper is organized as follows. The logarithm normalization restore method is introduced in Section 2. Section 3 analyzes the multi-wavelet analysis method. The detail realization method based on the logarithm computation and the multi-wavelet LH component feature is given in Section 4. The simulation experiments are done on the extended Yale B and CMU PIE Pose C09 face databases in Section 5. The conclusion is presented in Section 6.

2. Logarithm normalization preprocessing. According to the Lambertian illumination reflection model [6], the face pixel $\mathbf{F}(x, y)$ at the point (x, y) can be viewed as the multiplication between the reflection component $\mathbf{R}(x, y)$ and the illumination component

$\mathbf{I}(x, y)$:

$$\mathbf{F}(x, y) = \mathbf{R}(x, y) \times \mathbf{I}(x, y) \quad (1)$$

From Eq. (1), we can see that the observed face image is the original image corrupted by a multiplicative noise. For convenience, we perform the logarithm computation on two sides of Eq. (1) as follows.

$$\log[\mathbf{F}(x, y)] = \log[\mathbf{R}(x, y)] + \log[\mathbf{I}(x, y)] \quad (2)$$

Because the logarithm cannot be taken for zeros or negative numbers, we first normalize the original face image and add 1 to each pixel, and then perform the logarithm computation. At last, we normalize the logarithm value again for embodying the detail information of the logarithmic image. For simplicity, we denoted this preprocessing approach as LN. The calculation steps can be described as follows.

Step 1. The normalization process is performed on the observed face image using the following equation:

$$\mathbf{NF}(x, y) = \frac{\mathbf{F}(x, y) - F_{min}}{F_{max} - F_{min}} \cdot 255 + 1 \quad (3)$$

where $\mathbf{NF}(x, y)$ is the normalization value of the pixel $\mathbf{F}(x, y)$, F_{max} and F_{min} are the maximum and minimum values of the observed image \mathbf{F} , respectively. Obviously, $\mathbf{NF}(x, y)$ takes values between 1 and 256.

Step 2. Perform the logarithm computation and normalization on the image \mathbf{NF} based on Eq. (4):

$$\mathbf{LN}(x, y) = \frac{\log_{10}(\mathbf{NF}(x, y))}{\log_{10}(1 + 255)} \cdot 255 \quad (4)$$

where $\mathbf{LN}(x, y)$ is the normalization logarithm value of $\mathbf{NF}(x, y)$, which takes value between 0 and 255.

Taking four images (Fig. 1(a)) of size 192×168 from the extended Yale B face database as examples, we process each of them first with Eq. (3) and then Eq. (4). The corresponding results are shown in Fig. 1(b). From Fig. 1(b), we can see that the logarithm computation and normalization can decrease the illumination's effect and restore the image to some extent.

3. Multi-wavelet analysis. The multi-wavelet analysis [7] can reduce the redundancy between signals, easily deal with the boundary, obtain the better filtering performance with the shorter multi-wavelet filter, and effectively decrease the computation complexity.

It is called the multi-wavelet if the scale function and the wavelet function include several functions at the same time in the wavelet transform [7]. The r multiple continuous multi-scale and multi-wavelet functions can be presented respectively as $\Phi(t) = (\phi_1(t), \phi_2(t), \dots, \phi_r(t))^T$ and $\Psi(t) = (\psi_1(t), \psi_2(t), \dots, \psi_r(t))^T$, $r \in N$. If $\Phi(t)$ presents the r multiple multi-scale functions in the multi-resolution space $\{V_j\}_{j \in Z}$, then $\Psi(t)$ is the r multiple multi-wavelet functions in the orthogonal supplemental space $\{W_j\}_{j \in Z}$ of the sub-space $\{V_j\}_{j \in Z}$ under the sub-space $\{V_{j-1}\}_{j \in Z}$. If $\Phi(t-k)$, $k \in Z$ form the Riesz bases in the sub-space V_0 , $\Phi_{j,k}(t) = 2^{-j/2} \Phi(t/2^j - k)$, $j, k \in Z$ form the Riesz bases in the sub-space V_j , and $\dots \subset V_3 \subset V_2 \subset V_1 \subset V_0 \subset V_{-1} \subset \dots$, $\overline{\bigcup_{j \in Z} V_j} = L^2(R)$, $\bigcap_{j \in Z} V_j = \{0\}$, $V_j = V_{j+1} \oplus W_{j+1}$, the multi-scale and multi-wavelet

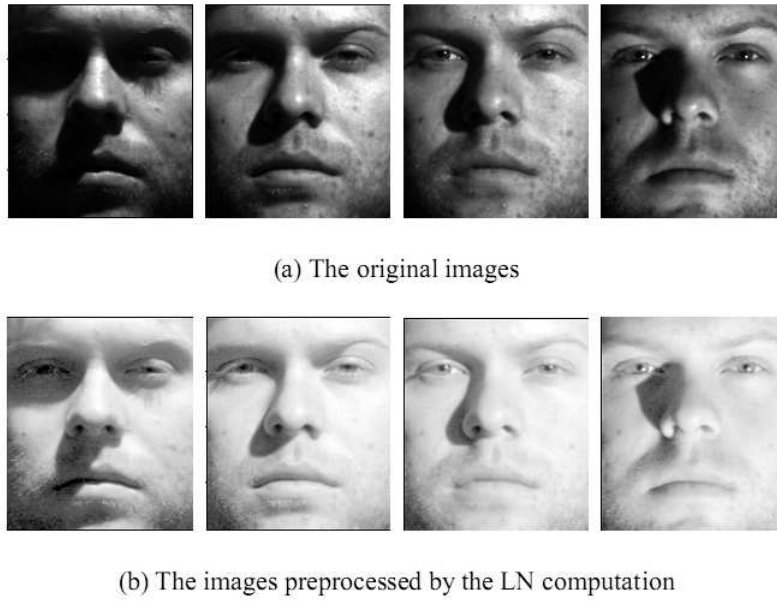


FIGURE 1. The original observing images and their preprocessed images by the LN computation

functions form the multi-resolution analysis in $L_2(R)$, which meet the following equations:

$$\Phi(t) = \sqrt{2} \sum_k \mathbf{H}_k \Phi(2t - k) \quad (5)$$

$$\Psi(t) = \sqrt{2} \sum_k \mathbf{G}_k \Psi(2t - k) \quad (6)$$

where $\mathbf{H}_{k \in Z} \in l^2(Z)^{r \times r}$ is the multi-scale filter coefficient matrix of size $r \times r$, and $\mathbf{G}_{k \in Z} \in l^2(Z)^{r \times r}$ is the $r \times r$ multi-wavelet filter coefficient matrix.

If $x(t) \in V_0 = V_1 \oplus W_1$, the analysis function of the orthogonal discrete multi-wavelet can be described as follows:

$$w_{j,k} = \sum_m \mathbf{G}_{m-2k} v_{j-1,m} \quad (7)$$

where $v_{j,k} = \langle x(t), \Phi_{j,k}(t) \rangle^T$ are scale coefficients, and $w_{j,k} = \langle x(t), \Psi_{j,k}(t) \rangle^T$ are wavelet coefficients.

The GHM orthogonal multi-wavelet function constructed using the fractal interpolation method by Geronimo et al. [9] is adopted in this paper.

4. Proposed scheme.

4.1. Multi-wavelet feature extraction and analysis of the face image. The input image should be pre-filtered to form the corresponding vector image before it is decomposed using the multi-wavelet filter because the multi-wavelet filter is a vector filter. Xia et al. [10] proposed two pre-filter methods: the Repeated Row pre-filter method (RR) and the Approximation Order pre-filter method (AO), which are used widely. The recognition effectiveness using these two pre-filter methods is similar, but the dimension of the feature using AO is only a quarter of that of the feature using RR, so we use the AO pre-filter method in this paper. After pre-filtering the input image, the multi-wavelet

decomposition is done. The overall process is shown in Fig. 2. First, the input image is preprocessed by the AO pre-filter method. And then the pre-filtered image is filtered by the row low and high pass multi-wavelet filters separately. Next, the image sampled down by 2 is filtered by the column low and high pass multi-wavelet filters separately. At last, the four feature components are gotten by sampling the filtered images down by 2, which are the LL, LH, HL and HH feature components.

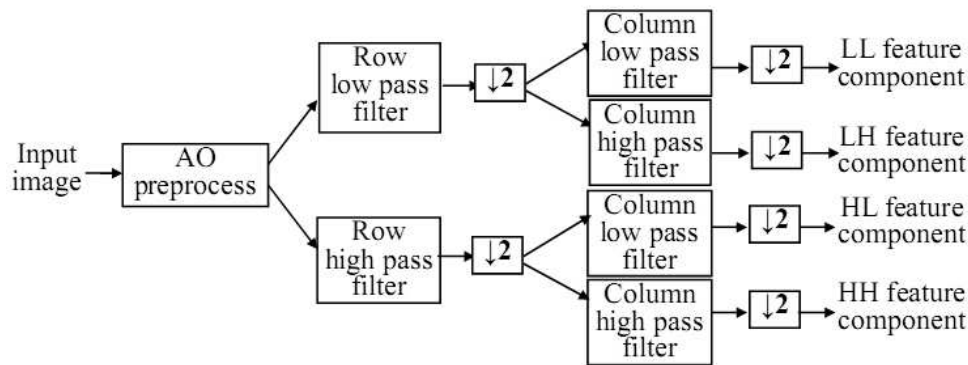


FIGURE 2. The multi-wavelet decomposition flow chart

For convenience, the size of all images is adjusted to 64×64 in the following experiments. Taking the first image in the Fig. 1(b) as an example, we decompose it by the GHM multi-wavelet function using the process shown in Fig.2. The four feature components are shown in Fig. 3. We can see that the LL feature component (Fig. 3 (a)) is the coarse information of the original image, which preserves the outline of the original image. The LH feature component (Fig. 3 (b)) preserves the edge detail of the original image in the vertical direction. The HL feature component (Fig. 3 (c)) preserves the edge detail of the original image in the horizontal direction. The HH feature component (Fig. 3 (d)) preserves the edge detail of the original image in the horizontal and vertical direction. The energy ratio of every feature component to the overall decomposition image is calculated and the results are shown in Table 1. From Table 1, we can see that the most energy of the signal is in the LL feature component, the next is in the LH feature component. The ratio of the HH feature component which mainly contains some noise is the least. So most of the works [1-5,7, 8] intended to take the low frequency component or the low frequency and band pass components as the feature and discarded the high frequency component. For analyzing the performance of every frequency band component better, we reconstruct the restored image from every single component feature by the inverse multi-wavelet transform and compute their amplitude spectrum separately, as shown in Fig. 4 and Fig. 5, in which we adjust the gray value to $0 \sim 255$ for observing clearly. From Fig. 4, we can see that the reconstructed image from LL (Fig. 4 (a)) loses the detail information of the original image. The reconstructed image from LH (Fig. 4 (b)) preserves the detail information of the original face image and filters the illumination effects better. The reconstructed image from HL (Fig. 4 (c)) contains the edge of the shadow caused by the illumination changes obviously. The reconstructed image from HH (Fig. 4 (d)) contains some high frequency noise, and their values are very small. By analyzing the amplitude spectrum in Fig. 5, it is clearly that the LH feature component contains more edge detail information. Therefore, we choose the LH multi-wavelet feature component as the feature in the proposed face recognition method in this paper.

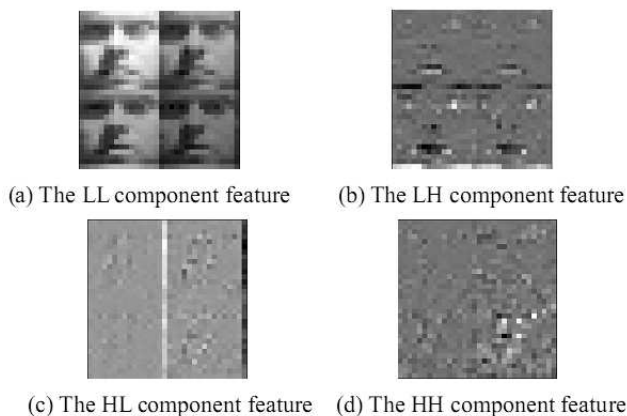


FIGURE 3. The image's multi-wavelet decomposition results

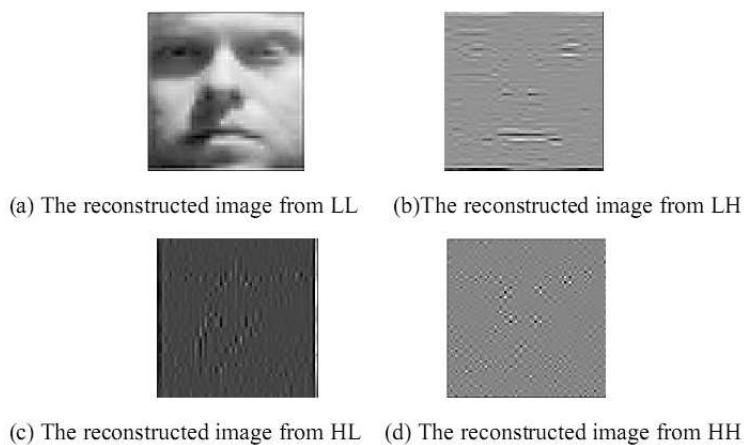


FIGURE 4. The reconstructed results from the image's multi-wavelet frequency band components

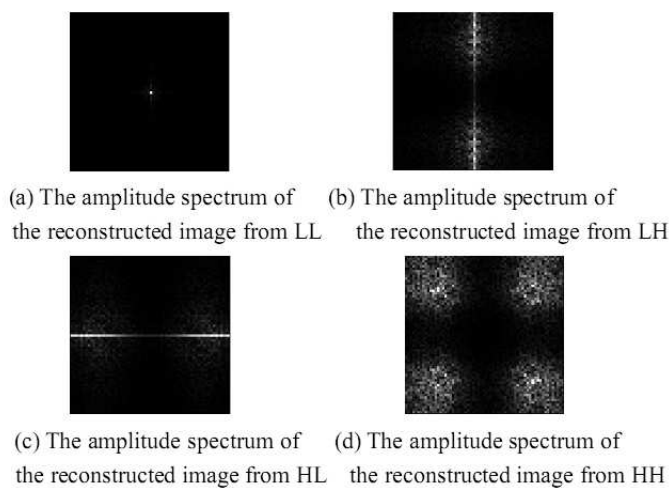


FIGURE 5. The amplitude spectrum figure of the reconstructed results of the image's multi-wavelet frequency band components

TABLE 1. The energy ratio of every frequency band component to the overall multi-wavelet decomposition image (%)

The frequency band component	LL	LH	HL	HH
The ratio of the energy	99.74	0.16	0.09	0.003

4.2. The proposed face recognition scheme based on the LN+multi-wavelet LH feature. The realization flow chart of the face recognition approach based on the logarithm computation and the multi-wavelet LH feature is shown in Fig.6. First, the input image is normalized. Next, the logarithm and normalization computation is performed. And then, the preprocessed image is pre-filtered using the AO pre-filter. Fourth, the pre-filtered image is filtered in row using the low pass multi-wavelet filter and in column using the high pass multi-wavelet filter sequentially. At last, the test face image is classified by the NN method. The detailed steps are as follows.

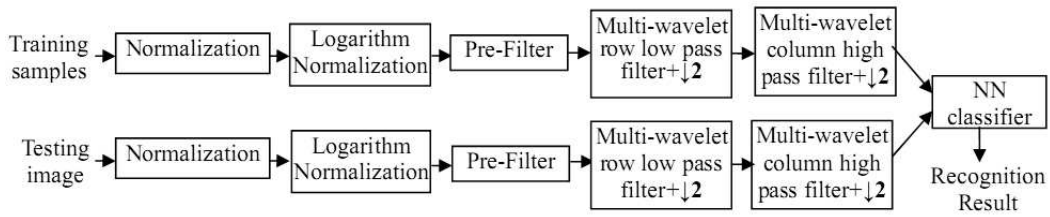


FIGURE 6. The face recognition algorithm flow chart based on the logarithm computation and the multi-wavelet LH feature

Step 1. Every face image \mathbf{F}_i in the training set is normalized using Eq. (3) to get the normalized image \mathbf{NF}_i , where N is the number of samples in the training set.

Step 2. The logarithm computation and normalization is performed on \mathbf{NF}_i using Eq. (4), and the result is denoted as \mathbf{LN}_i , $1 \leq i \leq N$.

Step 3. \mathbf{LN}_i is pre-filtered using the AO pre-filter [9], and the result is denoted as \mathbf{PLN}_i , $1 \leq i \leq N$.

Step 4. Every row of the \mathbf{PLN}_i is filtered using the multi-wavelet low filter and down sampled by 2 first, and then every column of the row filtered image is filtered using the multi-wavelet high filter and down sampled by 2. Thus, we can get the LH multi-wavelet feature \mathbf{MW}_i , $1 \leq i \leq N$. For description convenience, we call this feature as the LN+LH feature.

Step 5. The test image is processed using Steps (1)-(4) to get its LN+LH feature.

Step 6. The test face is recognized using the NN classifier.

5. Experimental results. In this paper, the simulation experiments are done on the extended Yale B face database [11] and the CMU PIE Pose C09 database [12]. The extended Yale B database is a classical face database with the variable illumination conditions, which contains 38 people and each has 64 images with different illumination conditions. The CMU PIE face database has 41368 images including 68 people with different poses, illuminations and expressions. We choose the face images with different illumination conditions in its sub-database Pose C09, which contains 1632 images and 24 images for every person.

5.1. Experiments on the extended Yale B database. In these experiments, we randomly select 1 to 16 face images from every person as the testing samples, respectively.

The rest images are taken as the testing samples. For convenience, we denote the used feature in the face recognition methods as the name of the method. We do 10 experiments for every situation using the face recognition methods based on the original images (OD), the logarithm normalization image (LN), the multi-wavelet LL features of the logarithm normalization image (LN+LL), the multi-wavelet LH features of the logarithm normalization image (LN+LH), the multi-wavelet LH features of the logarithm normalization image (LN+HL), the LL+sparse method(LLS) [8] and the LN+wavelet method(LNW) [4]. The parameter λ is chosen as 0.9, the size of the neighborhood window is 9×9 and the Haar wavelet is selected in the LN+wavelet method [4]. For evaluating every methods better, the average value of the recognition rates (AR) and their standard deviation (SR) are calculated, as shown in Table 2, where LN+LH presents the proposed method in this paper. From Table 2, we can see that the recognition rate of the proposed method is obviously better than that of the other methods. Especially the recognition effectiveness is improved for the small number of the training samples. By analyzing the relative value of the SR value, we can see that the proposed method has better robustness.

TABLE 2. The recognition rates and their standard variances with the methods using different features based on the extended Yale B database (%)

n^*	OD		LN		LN+LL		LN+LH		LN+HL		LLS[8]		LNW[4]	
	AR	SR	AR	SR	AR	SR	AR	SR	AR	SR	AR	SR	AR	SR
1	12.43	1.18	13.26	1.46	12.48	1.41	51.50	6.60	18.91	1.72	28.92	2.25	29.33	3.35
2	17.97	1.44	20.17	1.57	18.75	1.65	64.06	3.61	29.09	1.60	46.39	3.32	42.29	5.38
3	23.54	1.60	27.17	1.82	25.38	1.74	75.42	3.62	37.59	1.97	58.96	1.92	43.81	8.94
4	27.23	1.78	31.58	1.75	29.19	1.79	79.88	2.96	43.61	2.24	71.74	1.69	58.37	2.30
5	31.51	1.96	35.89	1.70	33.25	1.78	84.99	2.65	49.80	3.73	77.21	2.19	59.65	1.46
6	35.36	1.46	39.93	1.50	37.00	1.51	87.45	2.34	54.86	2.20	82.44	0.78	61.06	7.26
7	38.00	1.43	42.76	1.51	39.66	1.39	88.94	1.28	57.59	1.79	83.40	0.94	56.02	9.65
8	40.15	1.30	44.84	1.02	41.39	0.94	90.80	1.62	61.35	2.44	87.13	1.55	64.95	7.52
9	42.32	0.90	47.48	0.89	43.90	0.87	92.25	1.43	64.62	2.35	88.61	0.75	67.27	4.70
10	44.27	1.32	50.04	1.61	46.11	1.31	92.35	1.03	66.91	2.00	89.33	0.75	62.86	9.60
11	46.61	1.13	52.48	0.93	48.36	0.86	94.16	0.96	70.10	0.83	90.13	1.18	71.81	7.96
12	47.36	0.70	54.44	0.88	50.51	0.86	94.56	0.94	72.14	1.03	91.02	1.50	69.29	9.80
13	49.63	1.03	55.96	0.90	51.57	0.95	95.10	0.97	73.27	1.65	90.32	1.52	68.91	8.01
14	51.50	0.98	57.31	0.88	52.97	1.05	95.73	0.74	75.52	1.45	91.32	1.41	75.19	9.05
15	52.09	1.00	58.56	0.93	54.08	0.69	96.01	0.52	76.68	1.25	92.76	1.25	65.12	9.14
16	54.31	1.03	60.16	1.21	55.77	1.12	96.41	0.50	77.99	1.24	93.82	0.94	75.79	3.04

n^* : The number of training samples per person

5.2. Experiments on CMU PIE Pose C09 database. In these experiments, we randomly select 1 to 6 face images from every person as the testing samples, respectively. The rest images are taken as the testing samples. We do 10 experiments for every situation using the face recognition methods mentioned in Section 5.1. We calculate the AR and their SR values, as shown in Table 3. From Table 3, we can see that the recognition effectiveness of the proposed method is better than that of the other methods, and has better robustness. Especially, it also has better performance for the small number of the training samples as the extended Yale B database. Although the recognition results using the LL+Sparse method [8] is similar to the results using the proposed LN+HL method

when the number of the training samples is big, the LL+Sparse method costs much time and has worse robustness.

TABLE 3. The recognition rates and their standard variances with the methods using different features based on the CMU PIE Pose database (%)

n^*	OD		LN		LN+LL		LN+LH		LN+HL		LLS[8]		LNW[4]	
	AR	SR	AR	SR	AR	SR	AR	SR	AR	SR	AR	SR	AR	SR
1	18.01	0.76	21.69	1.07	19.94	0.89	71.66	3.64	34.16	1.80	52.92	1.88	21.59	1.11
2	30.03	1.20	35.82	0.88	33.16	0.94	83.59	2.08	53.22	2.32	78.40	2.75	35.51	1.07
3	39.54	1.53	46.92	1.60	43.59	1.21	87.83	0.80	65.16	2.55	85.97	1.60	46.83	1.35
4	47.43	1.90	55.86	1.32	51.81	1.25	89.20	0.91	73.20	2.06	88.76	1.21	54.61	1.47
5	53.94	1.78	61.88	1.48	58.21	1.41	89.58	0.57	77.14	2.03	89.38	1.35	61.95	1.31
6	60.37	1.21	67.98	2.14	64.40	1.51	90.20	0.59	81.03	1.45	90.10	1.24	67.04	1.10

n^* : The number of training samples per person

6. Conclusions. By studying the illumination model of the image and every multi-wavelet component feature, the face recognition based on the logarithm computation and the multi-wavelet LH feature is proposed. First, the multiplicative illumination noise of the image corrupted by illumination is transformed into the additive noise by the logarithm computation. Next, the preprocessed image is pre-filtered using the corresponding pre-filter of the multi-wavelet. And then the pre-filtered image is filtered by the low pass multi-wavelet filter in row and by the high pass multi-wavelet filter in column sequentially. At last, the face is recognized by the NN method. The experiments using the face recognition method based on OD, LN, LN+LL, LN+LH, LN+HL features, the LL+sparse method [8] and the LN+wavelet method [4] are performed on the extended Yale B face database and the CMU PIE Pose C09 database. The experimental results show that the proposed method can effectively improve the recognition rate and has better robustness. In addition, it can solve the problem of the small number of training samples better.

REFERENCES

- [1] D. Shan, R. Ward, Wavelet-based illumination normalization for face recognition, *Proce. of the 2005 IEEE International Conference on Image Processing*, Piscataway, vol. 2, pp. 954-957, 2005.
- [2] Y. Z. Goh, A. B. J. Teoh, M. K. O. Goh, Wavelet based illumination invariant preprocessing in face recognition, in *2008 Congress on Image and Signal Processing*, vol. 3, pp. 421-425, 2008.
- [3] X. Cao, L. G. Yu, J. Y. Yang, Illumination invariant face recognition based on wavelet transform and denoising model, *Journal of Computer Application*, vol. 31, no. 8, pp. 2126-2129, 2011.
- [4] X. Cao, W. Shen, L.G. Yu, Y. L. Wang, J.Y. Yang, Z.W. Zhang, Illumination invariant extraction for face recognition using neighboring wavelet coefficients, *Pattern Recognition*, vol. 45, no.4, pp.1299-1305, 2012.
- [5] X. F. Nie, Z. F. Tan, J. Guo, Application of wavelet packet transform for illumination compensation in face recognition, *Opto-Electronic Engineering*, vol. 35, no.1, pp. 50-54, 2008.
- [6] B. K. P. Horn, *Robot vision*, MIT press, Cambridge, MA, 1997.
- [7] T. N. T. Goodman, S. L. Lee, Wavelets of multiplicity r , *Transactions of the American Mathematical Society*, vol. 342, pp. 307-324, 1994.
- [8] L. J. Zhou, Y. K. Xu, Z. M. Lu, T. Y. Nie, Face recognition based on multi-wavelet and sparse representation, *Journal of Information Hiding and Multimedia Signal Processing*, vol. 5, no. 3, pp. 406-414, 2014.
- [9] J. M. Geronimo, D. P. Hardin, P. R. Massopust, Fractal functions and wavelet expansions based on several scaling functions, *Journal of Approximation Theory*, vol. 78, no.3, pp.373-401, 1994.

- [10] X. G. Xia, J. S. Geronimo, et al. , Design of prefilters for discrete multiwavelet transforms, *IEEE Transactions on Signal Processing*, vol. 44, no.1, pp. 273-298, 1996.
- [11] K. C. Lee, J. Ho, D. J. Kriegman, Acquiring linear subspaces for face recognition under variable lighting, *IEEE Transactions on Pattern Analysis and Machine Intelligence*, vol. 27, no. 5, pp. 684-698, 2005.
- [12] T. Sim, S. Baker, M. Bsat, The CMU pose, illumination, and expression database, *IEEE Transactions on Pattern Analysis and Machine Intelligence*, vol. 27, no.12, pp. 1615-1618, 2003.